Radiative jets from variable sources

A. Raga, J. Canto, F. de Colle, P. Kajdic, A. Esquivel, P. Velazquez, A. Rodriguez

(the “chilango boys”)

Some of the groups active in modeling variable jets

E. de Gouveia Dal Pino, A. Cerqueira (→Ipanema)

S. Cabrit, T. Downes (→ coiffeur)

M. Smith, A. Rosen (→ ?????)

T. Gardiner, A. Frank (→ enstein)

A. Ferrari +++ (→ mafia di Torino)

a. Characteristics of the variable ejection

→ Pulsed: 54

→ Precessing: 21

→ Orbiting: 21

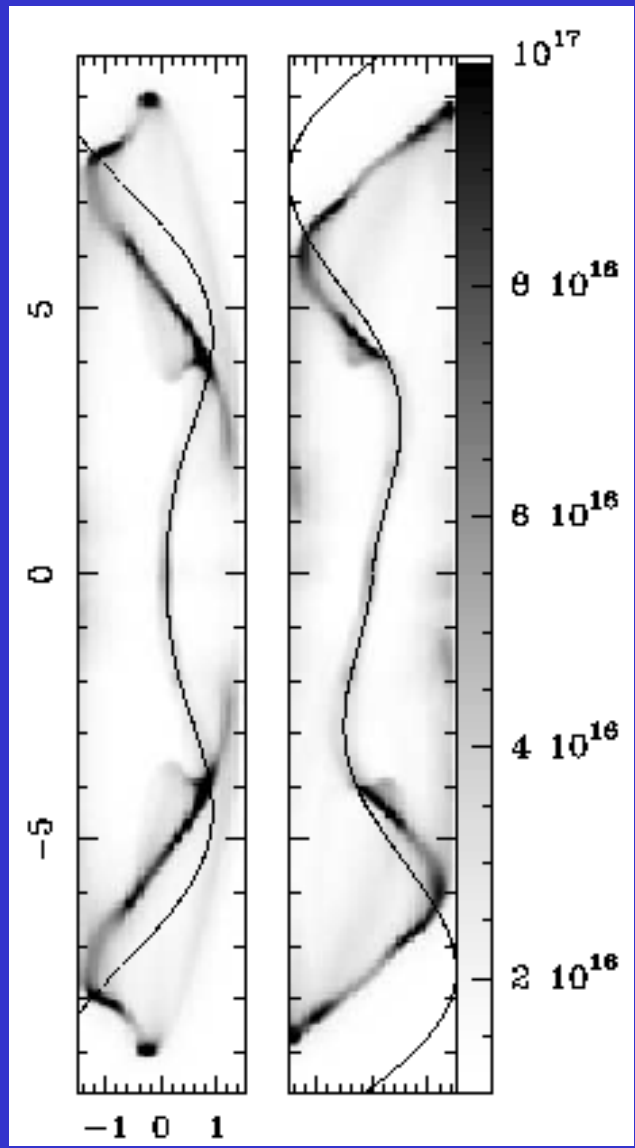

Masciadri & Raga 2002

b. Technique

→analytic: 13

→1D sims: 6

→ slab sims: 5

→ axisymmetric sims: 21

→ 3D sims: 37

→ MHD: 10

Raga & Kofman 1992

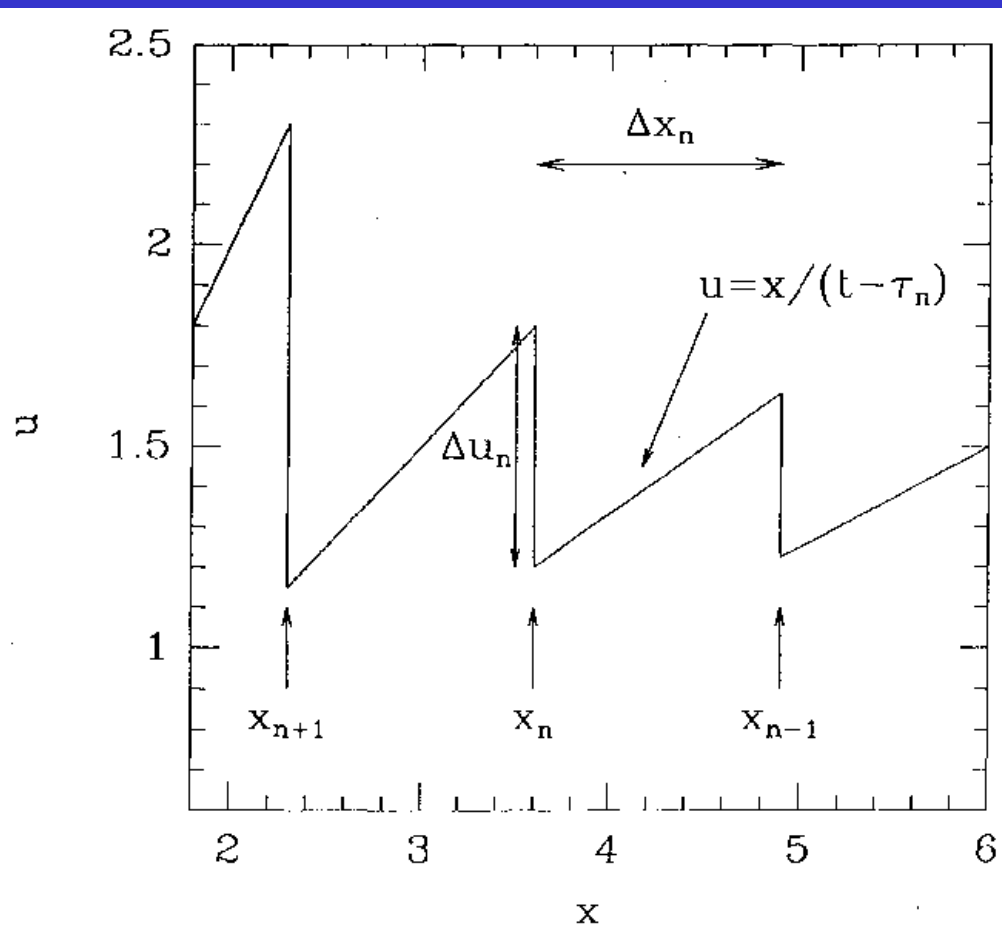

c. predictions

→ halpha: 23

→ other lines: 25

→ intensity maps: 25

→ line profiles: 4

→ pos-vel diagrams: 10

→ velocity channel maps: 5

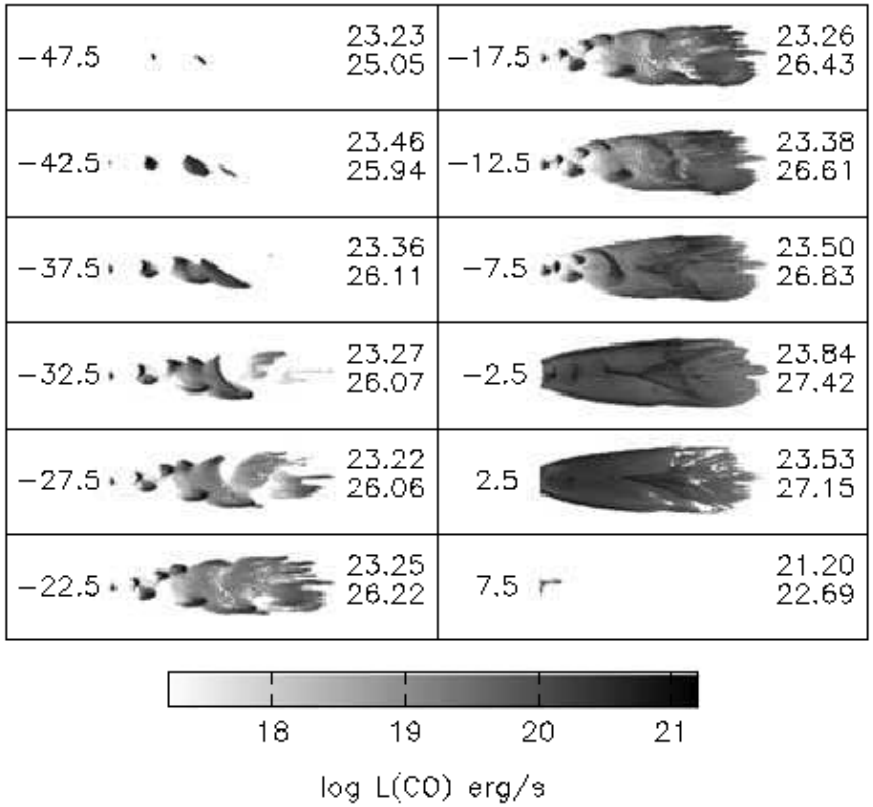

Rosen & Smith 2004

d. Specific objects

→total: 12

→ HH 34: 4

→ HH 111: 2

→ HH 32: 1

→ HH 30: 1

→ HH 110: 1

→ DG Tau: 2

→ HH 505: 1

→ HH 555: 1

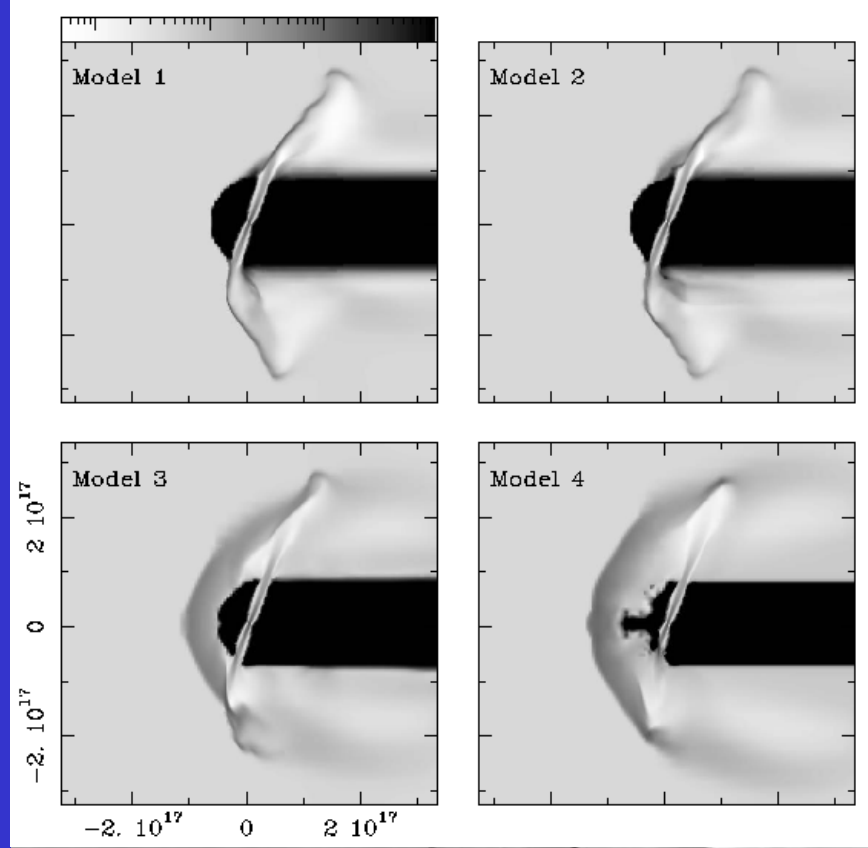

e. special dynamical or microphysical situations

→ collision with dense cloud(s): 4

→ stratified environment: 3

→ molecular jet/environment: 14

→ photoionised jets: 6

→ giant jets: 3

→ jet in sidewind: 3

jet in sidewind:

Masciadri & Raga 2001

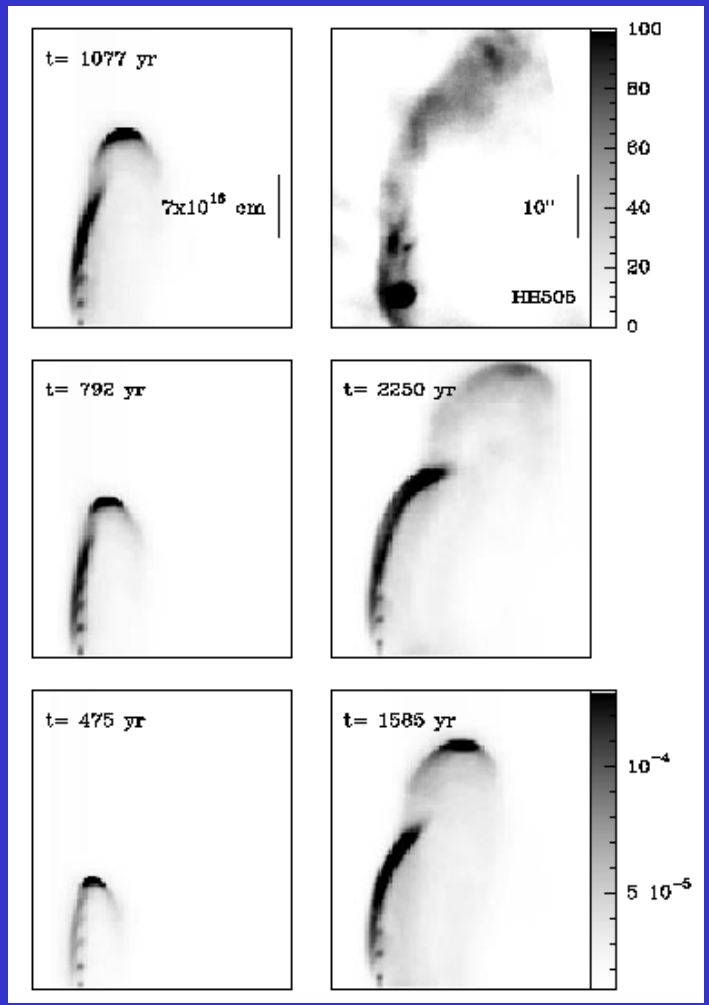

Ciardi et al. 2008

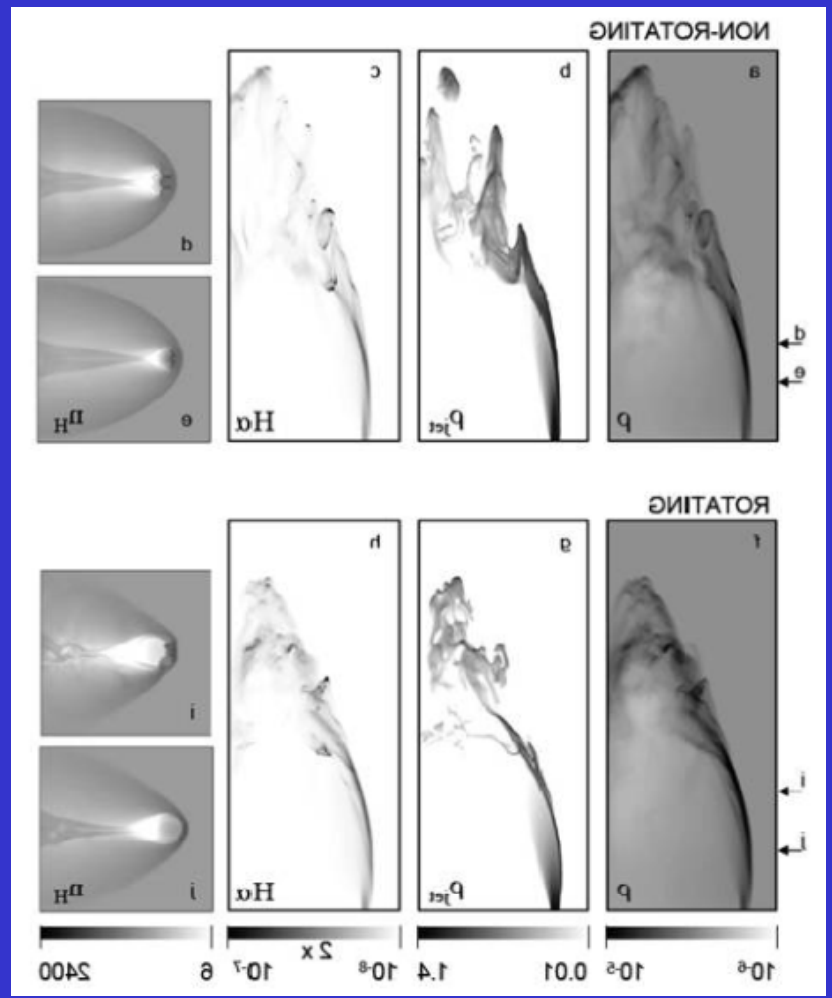

externally photoionized jet

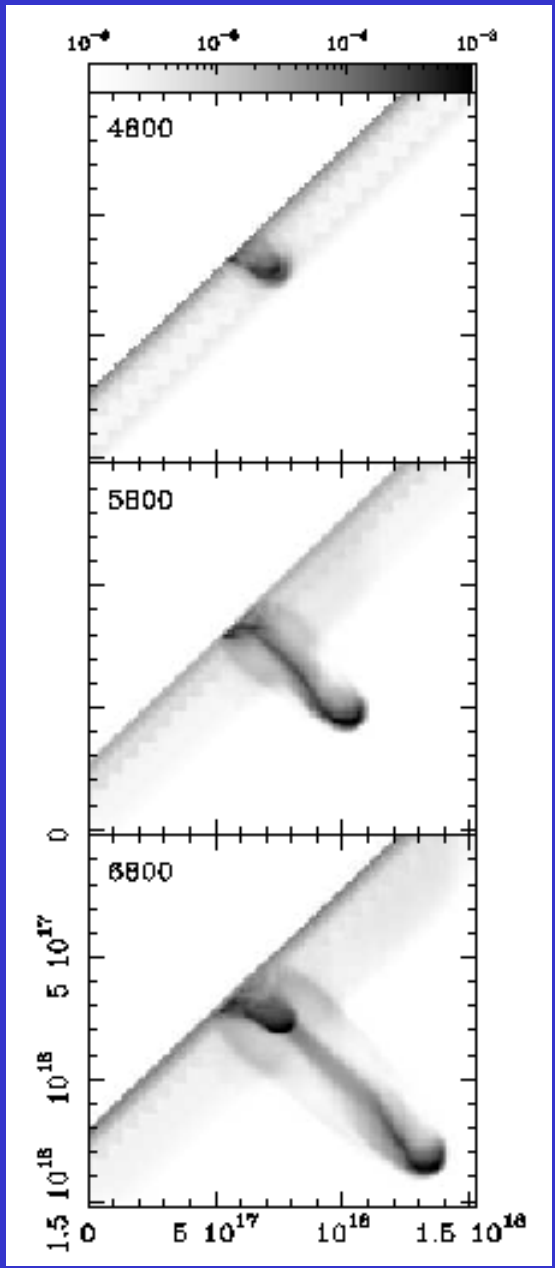

Raga & Reipurth 2004

conference poster

This talk: 2 and 3D simulations illustrating

→2 vs. 3D

→Non-top hat initial velocity cross section

→Initial opening angle of jet

→Ejection velocity variability

→Precession

All simulations have a single species network (HI/II), and a parametrized cooling function

2D vs. 3D: head of a top-hat jet

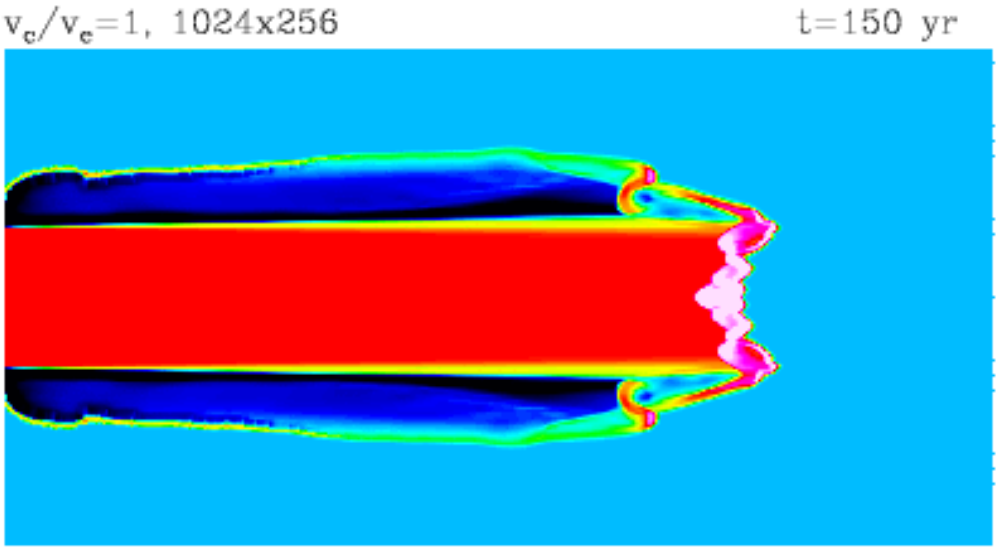

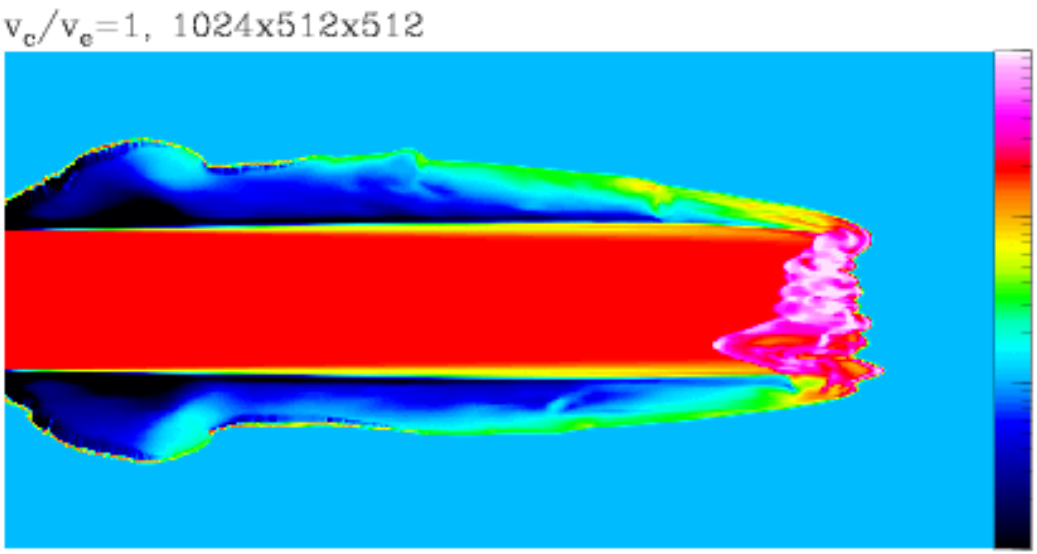

→ 6-level, binary adaptive grid

(**2D:** 1024×256, **3D:** $1024 \times 512 \times 512$ at maximum resolution)

→ size of domain along axis: 10^{17} cm

→ jet radius: $r_j = 7 \times 10^{15}$ cm

→ jet radius resolved with 71 grid points

→ $v_j = 200$ km s^{-1}, $n_j = 1000$ cm^{-3}, $T_j = 1000$ K

→ $n_{env} = 50$ cm^{-3}, $T_{env} = 100$ K

→ 3D simulation with a sinusoidal density perturbation with wavelength of $r_j/2$ and half-amplitude of 5 %

2D vs. 3D: the head of a non-top hat jet

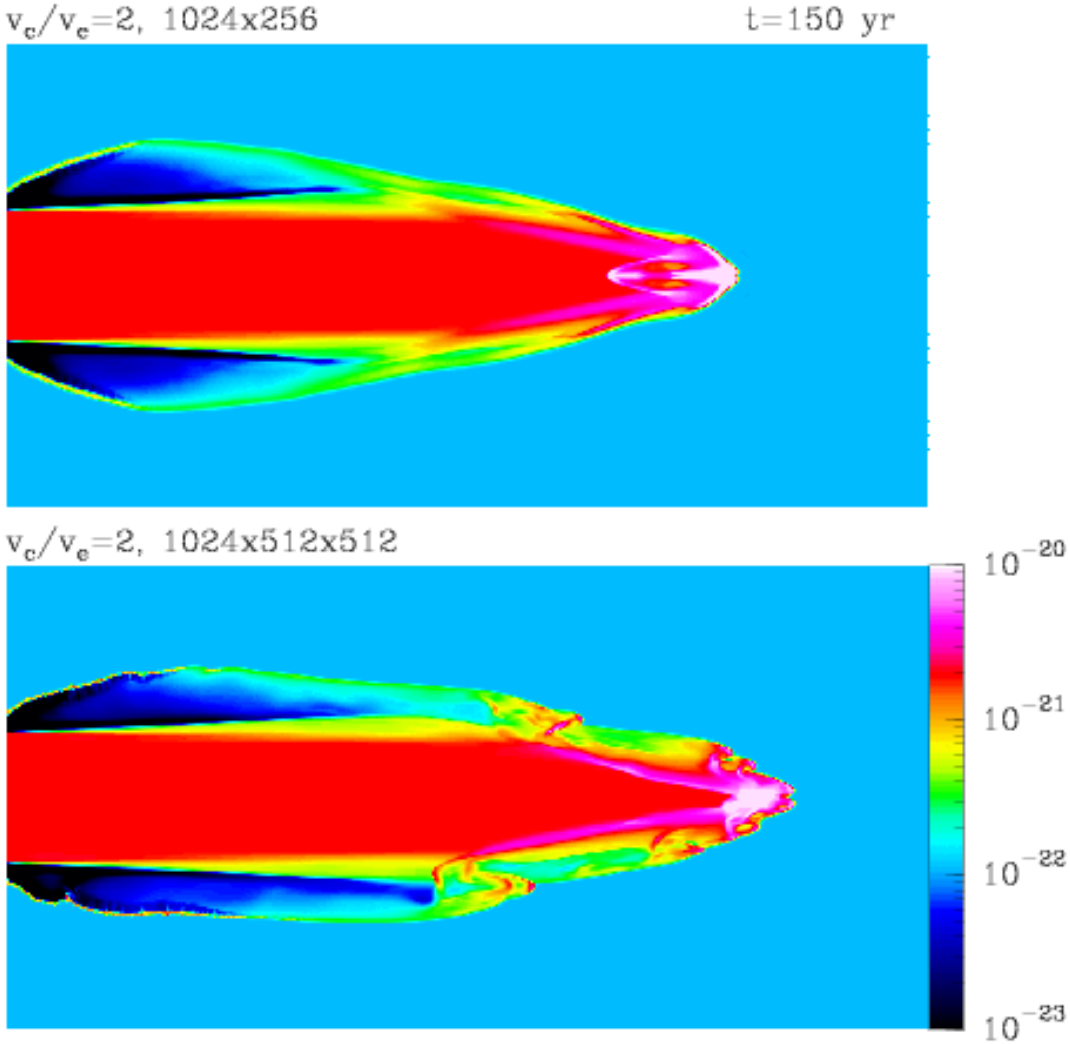

$\rightarrow$ the same as previous model but with a quadratic

injection velocity profile with $v_c/v_e = 2$

The effect of a non-zero initial opening angle

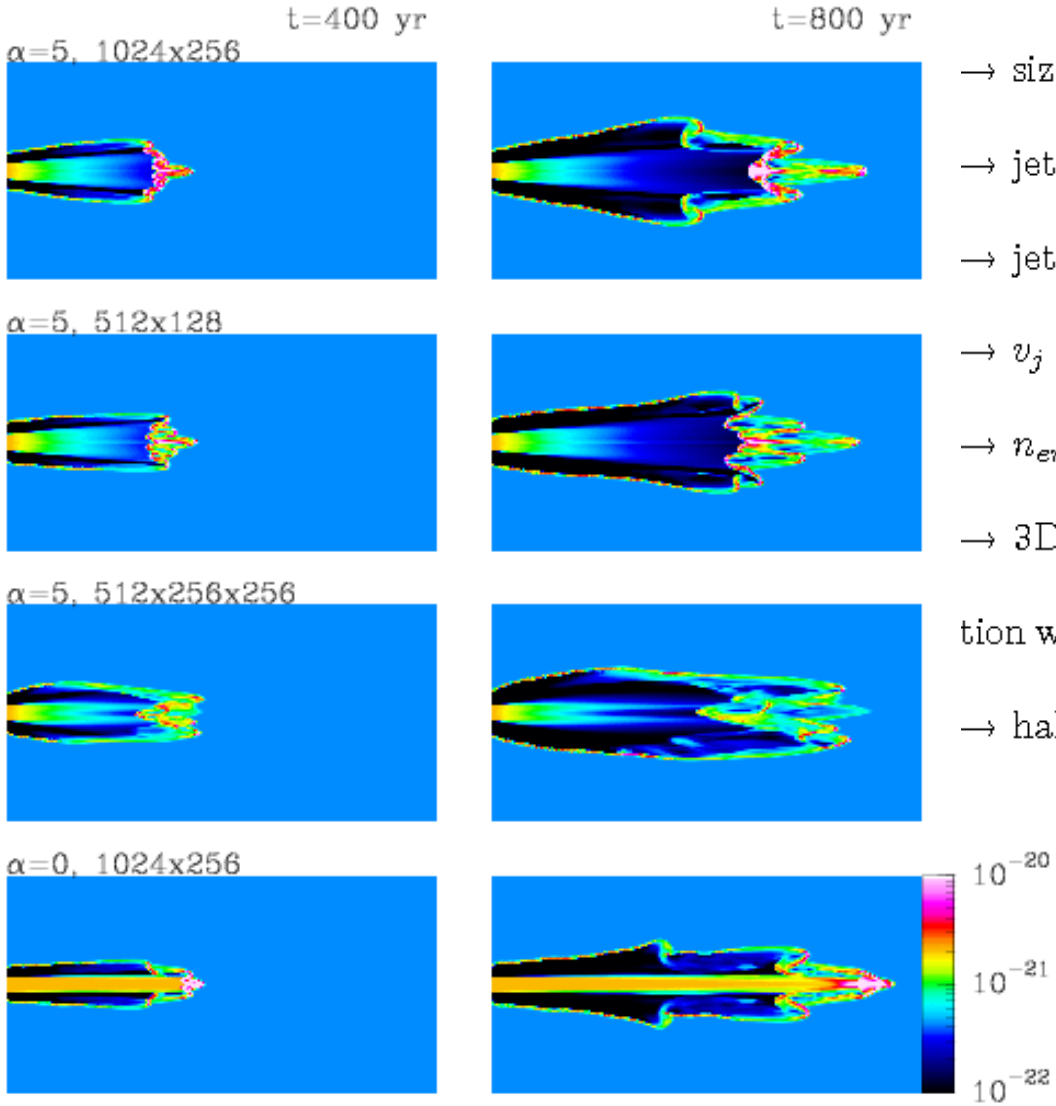

→ size of domain along axis: 4×10^{17} cm

→ jet radius: $r_j = 7 \times 10^{15}$ cm

→ jet radius resolved with 9 or 18 grid points

→ $v_j = 200$ km s^{-1}, $n_j = 1000$ cm^{-3}, $T_j = 1000$ K

→ $n_{env} = 200$ cm^{-3}, $T_{env} = 100$ K

→ 3D simulation with a sinusoidal density perturbation with wavelength of $r_j/2$ and half-amplitude of 5 %

→ half-opening angle $\alpha = 0, 5°$

The effect of a non-zero initial opening angle

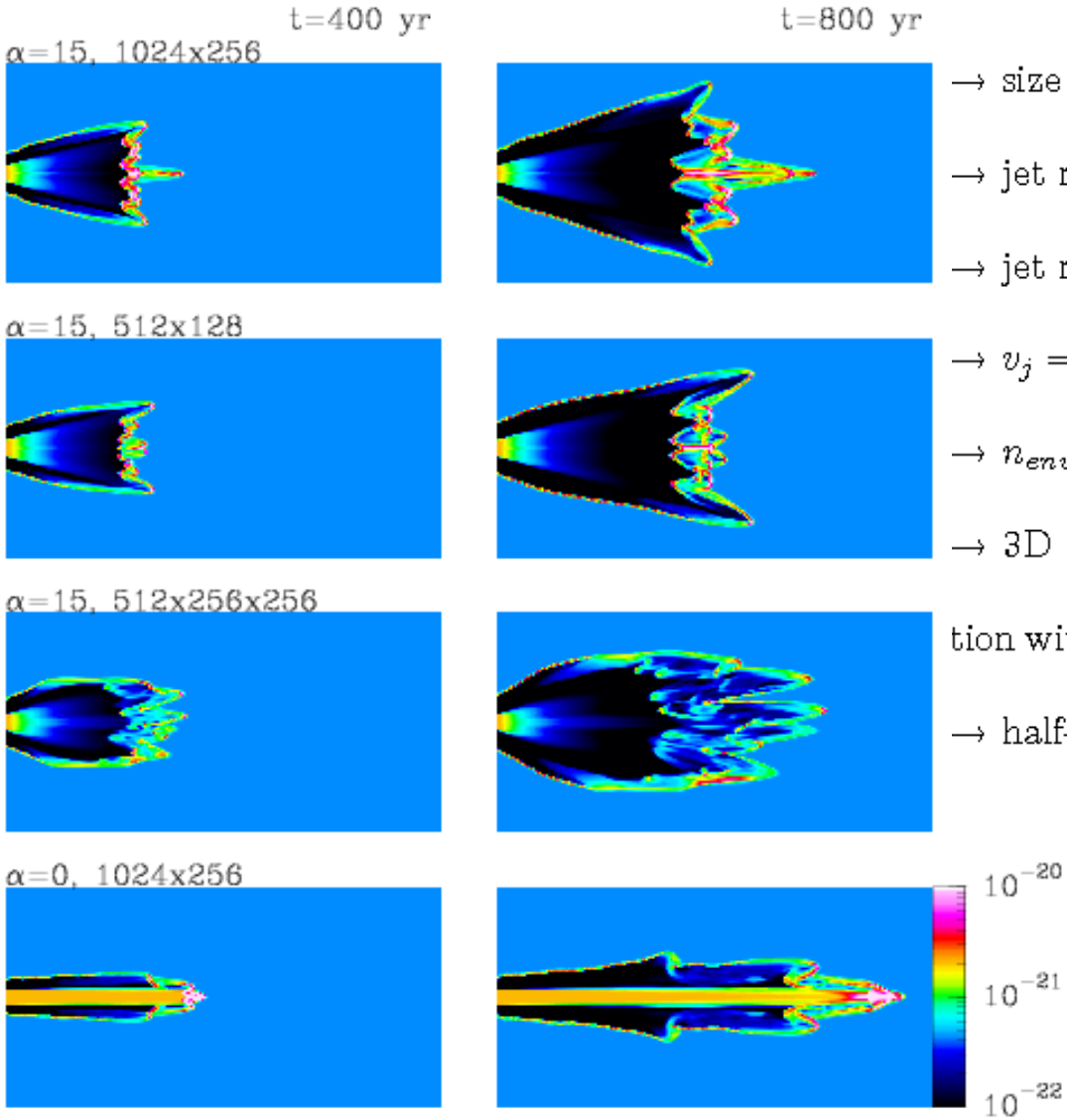

→ size of domain along axis: 4×10^{17} cm

→ jet radius: $r_j = 7 \times 10^{15}$ cm

→ jet radius resolved with 9 or 18 grid points

→ $v_j = 200$ km s^{-1}, $n_j = 1000$ cm^{-3}, $T_j = 1000$ K

→ $n_{env} = 200$ cm^{-3}, $T_{env} = 100$ K

→ 3D simulation with a sinusoidal density perturbation with wavelength of $r_j/2$ and half-amplitude of 5 %

→ half-opening angle $\alpha = 0$, 15°

Models with an ejection velocity variability

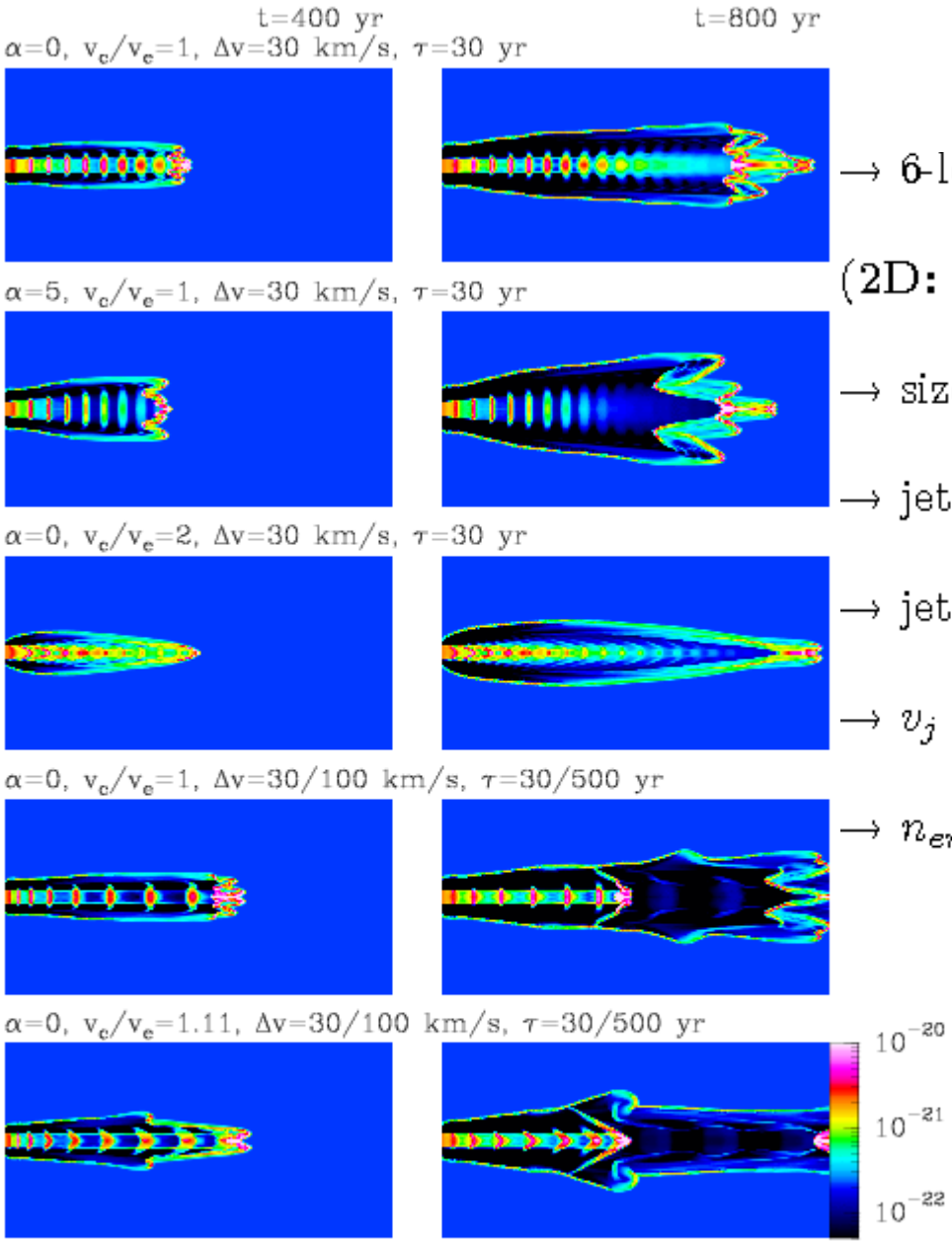

→ 6-level, binary adaptive grid

(**2D:** 1024×256)

→ size of domain along axis: 4×10^{17} cm

→ jet radius: $r_j = 7 \times 10^{15}$ cm

→ jet radius resolved with 18 grid points

→ $v_j = 200$ km s^{-1}, $n_j = 1000$ cm^{-3}, $T_j = 1000$ K

→ $n_{env} = 100$ cm^{-3}, $T_{env} = 100$ K

Top-hat jet with ejection velocity variability: the movie

$\rightarrow$ 6-level, binary adaptive grid

(**2D:** 1024×256)

$\rightarrow$ size of domain along axis: 4×10^{17} cm

$\rightarrow$ jet radius: $r_j = 7 \times 10^{15}$ cm

$\rightarrow$ jet radius resolved with 18 grid points

$\rightarrow$ $v_j = 200$ km s^{-1}, $n_j = 1000$ cm^{-3}, $T_j = 1000$ K

$\rightarrow$ $n_{env} = 100$ cm^{-3}, $T_{env} = 100$ K

$\rightarrow$ **two sinusoidal modes:**

$\Delta v = 30$ km s^{-1}, $\tau = 30$ yr

$\Delta v = 100$ km s^{-1}, $\tau = 500$ yr

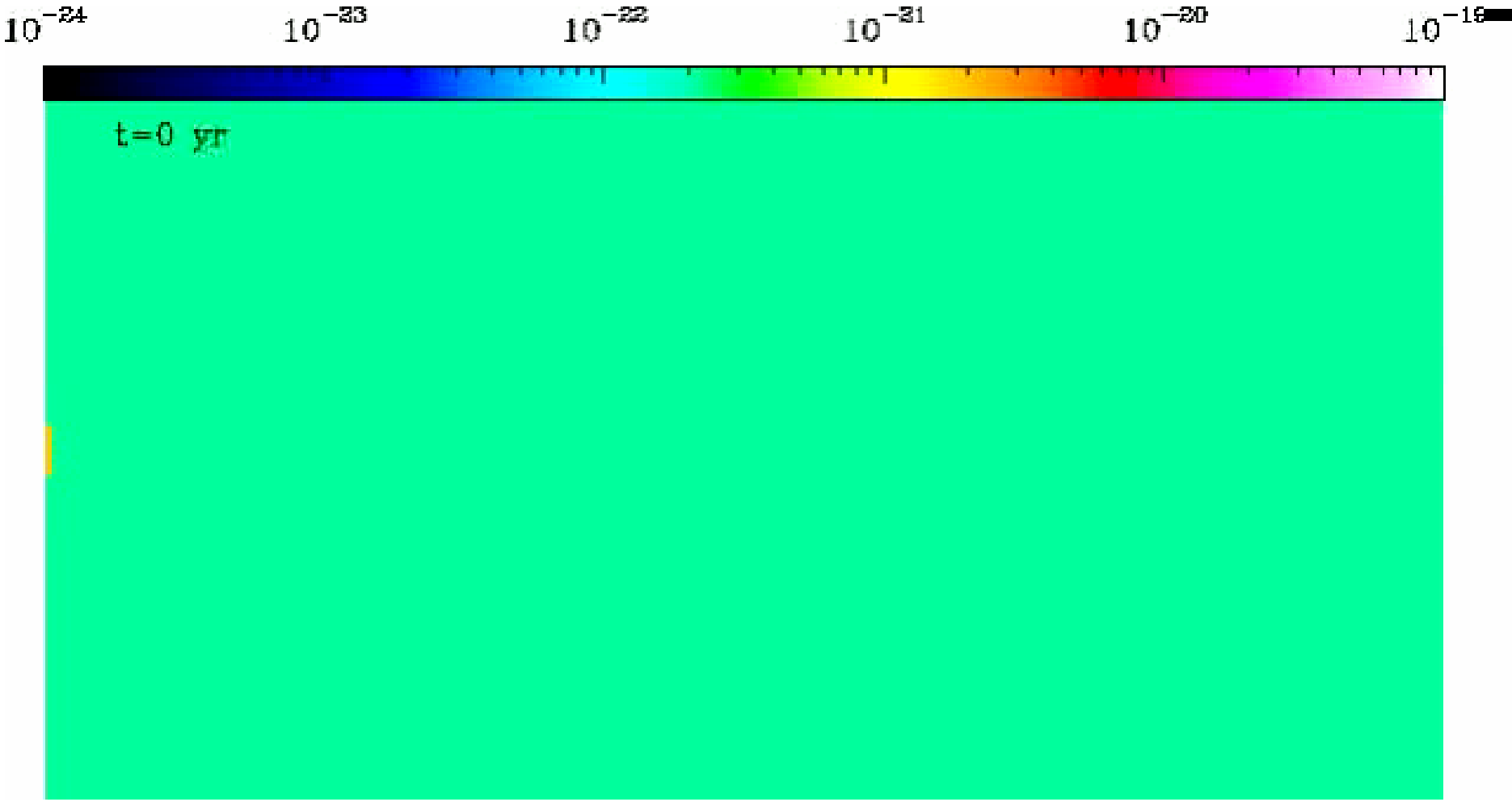
10^{-24}
10^{-23}
10^{-22}
10^{-21}
10^{-20}
10^{-19}
t=0 yr

Non-sinusoidal modes

$$f(t) = 1 + \cos(2\pi t/\tau)$$

$$f_c(t) = f(t) - 1$$

$$f_l(t) = 0.142\ f(t)\ e^{-10t/\tau} - 1$$

$$f_r(t) = 0.142\ f(t)\ e^{10t/\tau} - 1$$

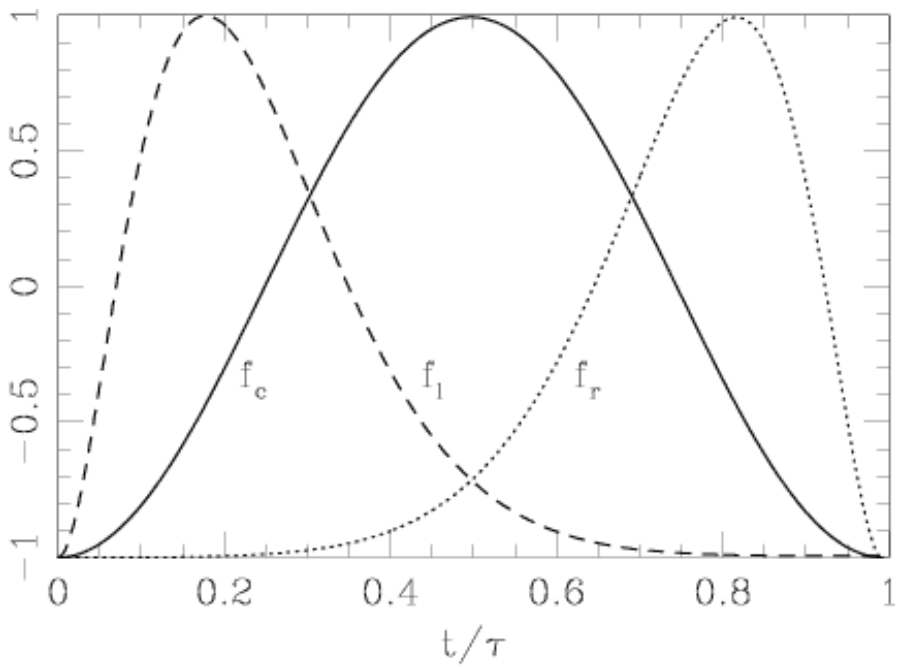

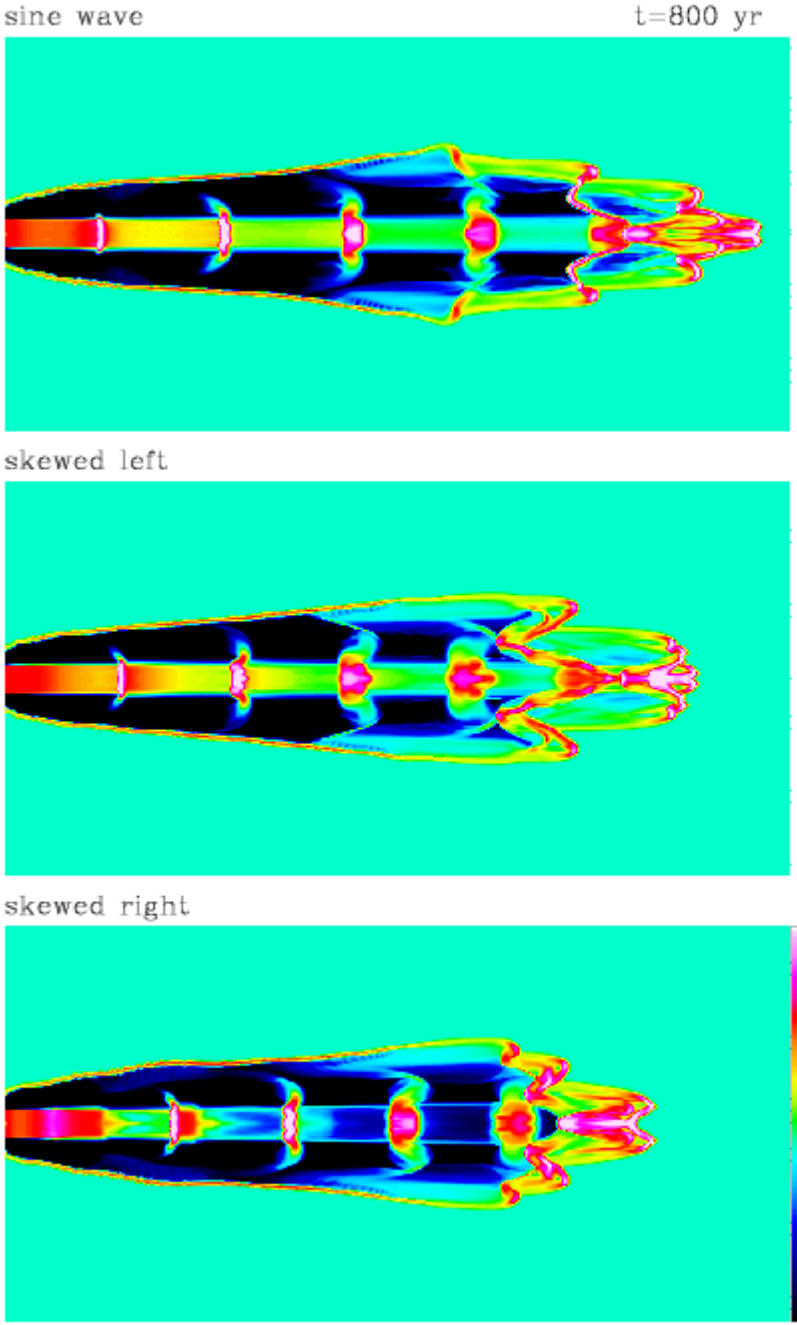

$\rightarrow$ size of domain along axis: 4×10^{17} cm

$\rightarrow$ jet radius: $r_j = 7 \times 10^{15}$ cm

$\rightarrow$ jet radius resolved with 18 grid points

$\rightarrow$ $v_j = 200$ km s^{-1}, $n_j = 1000$ cm^{-3}, $T_j = 1000$ K

$\rightarrow$ $n_{env} = 100$ cm^{-3}, $T_{env} = 100$ K

$\rightarrow$ single-mode variability with $\Delta v = 50$ km s^{-1} and

$\tau = 100$ yr

Ejection velocity variability + precession

3D: $1024 \times 512 \times 512$

$\rightarrow$ size of domain along axis: 4×10^{17} cm

$\rightarrow$ jet radius: $r_j = 7 \times 10^{15}$ cm

$\rightarrow$ jet radius resolved with 18 grid points

$\rightarrow$ $v_j = 200$ km s^{-1}, $n_j = 1000$ cm^{-3}, $T_j = 1000$ K

$\rightarrow$ $n_{env} = 100$ cm^{-3}, $T_{env} = 100$ K

$\rightarrow$ **two sinusoidal modes:**

$\Delta v = 20$ km s^{-1}, $\tau = 30$ yr

$\Delta v = 100$ km s^{-1}, $\tau = 230$ yr

$\rightarrow$ **precession:** $\tau_{prec} = 1000$ yr, half-angle: $5°$

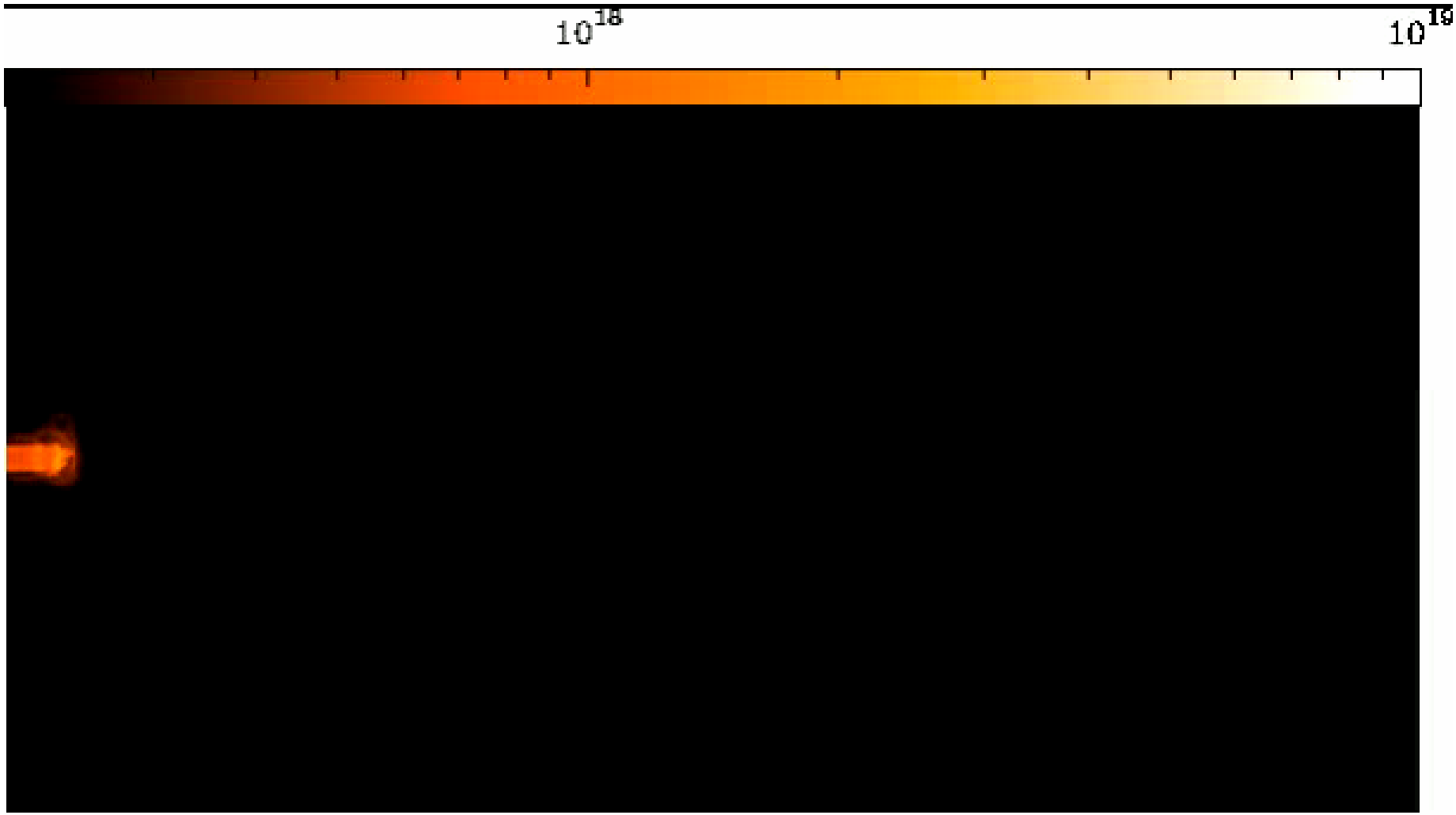
10^{18}
10^{19}
t=50 yr

Summary:

→ Models of jets with variable ejections have been explored in unprecedented detail

→The structures of some HH objects can be reproduced very well with variable jet models

→The jet structure depends on:

- → the amplitudes and periods
- → the initial cross section

→The precise functional form of the variability appears to be less important

→Precession (and/or orbital motion) can play an important role